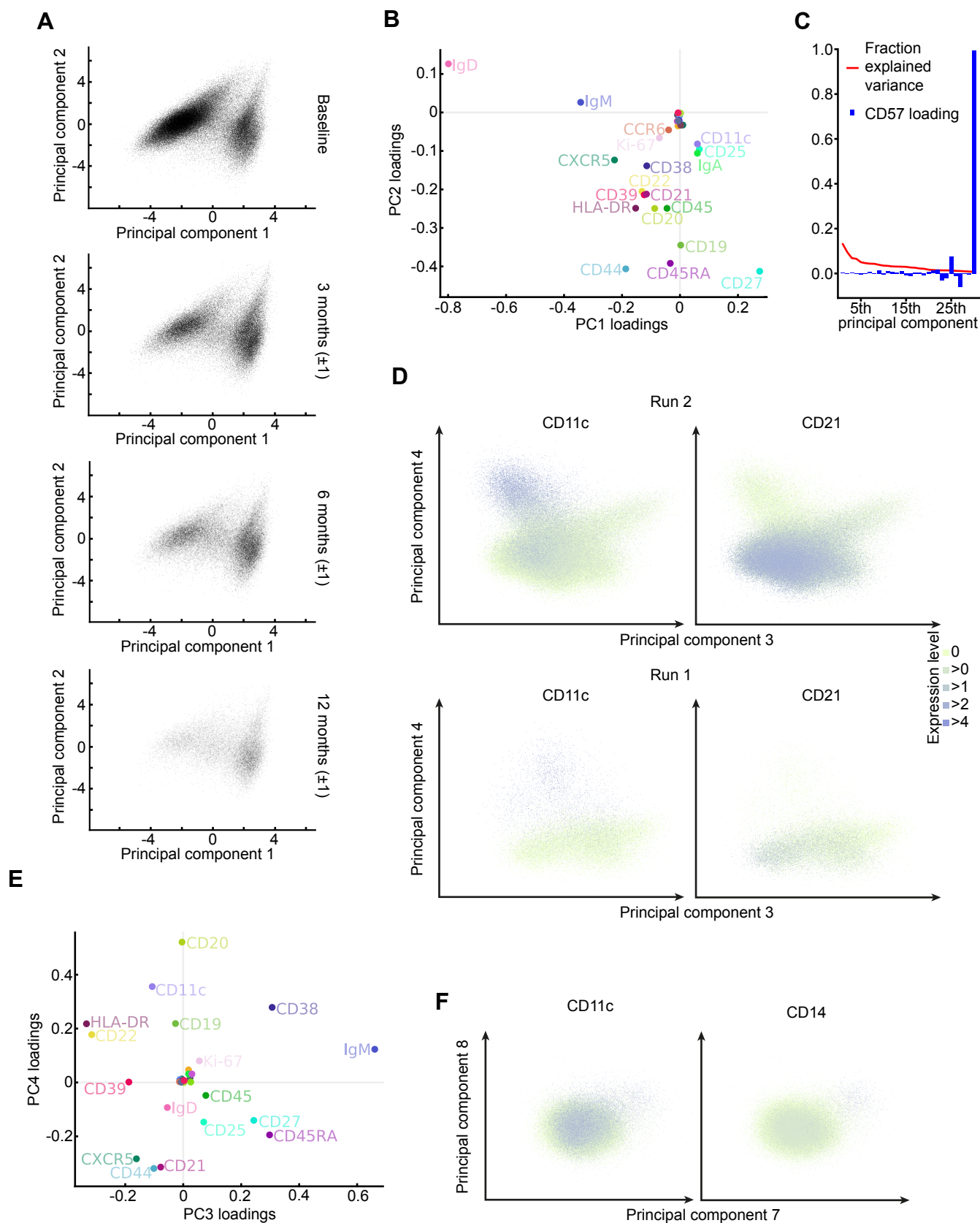


**Figure S1**

Healthy control and characterisation of CD11c<sup>+</sup> clusters. (A–B) t-SNE for all cells from 1 healthy donor. (C) t-SNE plot of B cells from all follow-up occasions in 18 patients (second run) using a maximum of 500 cells per sample. CD57 and CD11c expression distributes into distinct clusters (lower right). (D) Reverse cumulative distributions of CD11c mass cytometry signal in B cells, with red curves representing run1 patients, blue run2 patients and green run2 healthy control. (E) Violin plots depicting the grade of marker expression (yellow) on the B cell cluster #26 delineated in Figure 1B. The marker expression on the remaining B cells is also displayed for comparison (pink). Width indicates the frequency of the expression level shown on the y-axis.



**Figure S2**

Principal component analysis. (A–B) Just like Figure 2A, the expected relative disappearance of naïve B cells in comparison to memory B cells is visible in PCA. Samples from the 2nd machine run are shown. The markers that drive the axes in B are shown in C. (C) The contribution of CD57 to the 30 principal components (run 2 data), showing that it is left to the last components which contain the least data. (D–E) The fourth principal component separates CD11c<sup>+</sup> cells from CD21<sup>+</sup> cells, in line with the existence of a CD11c<sup>+</sup>CD21<sup>-</sup> cluster in the t-SNE analysis. There is a clear second group of CD21<sup>-</sup> cells in the plot, these are characterised by CD38 and IgM expression, as can be seen in D. (F) CD14<sup>+</sup>CD11c<sup>+</sup> cells are visible in the 7th principal component of run 2. A similar shift was seen of PC7 for run 1 (data not shown).

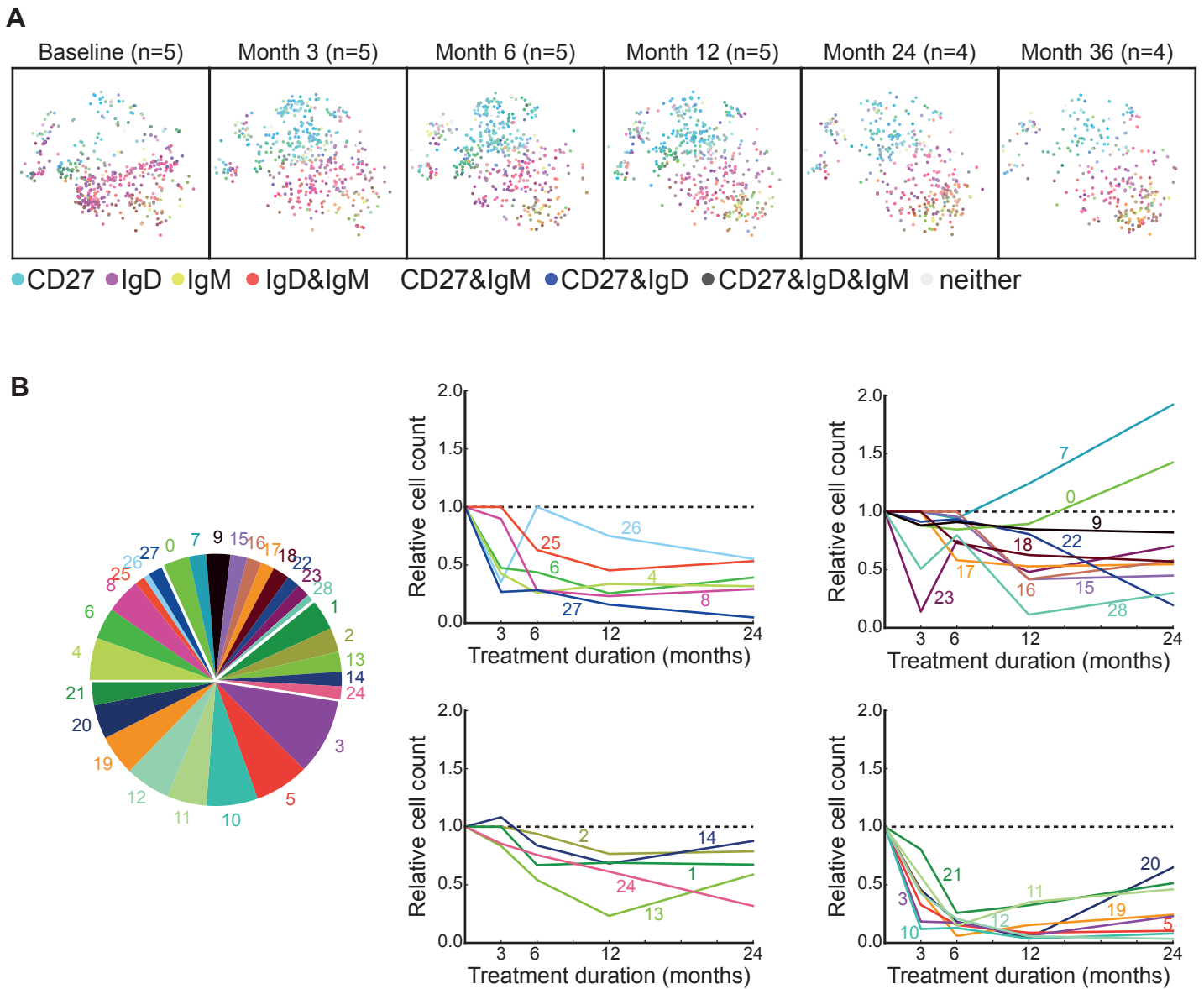


**Figure S3**

B cell cluster alterations over time. (A) t-SNE plots of B cells from each follow-up occasion (100 cells per sample) in five patients (pilot run). (B) Pie chart of the relative size of the clusters at baseline, and graphs illustrating relative cell count alterations during follow-up compared to baseline values in each one of the B cell clusters delineated in the t-SNE plot of Figure 1B. The clusters are split into four plots for illustrative purposes, according to the approximate location of the cluster in the plot of Figure 1A: CD57<sup>+</sup> and CD11c<sup>+</sup> located at the top of it (e.g. cluster 4); then switched memory (e.g. cluster 0); then activated, pre-switching and double-negative memory (e.g. cluster 1); then naïve at the bottom of it (e.g. cluster 3).

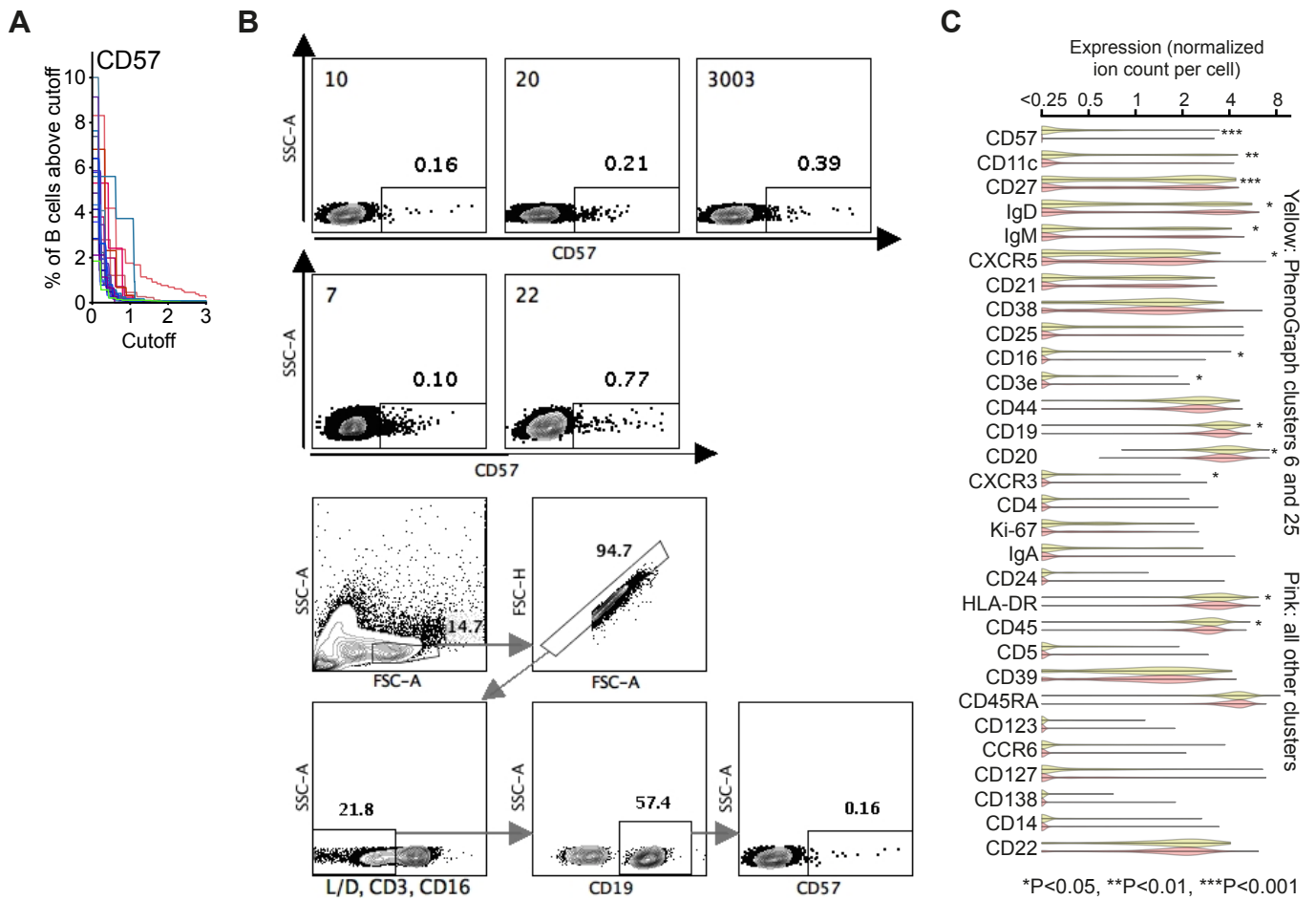


#### Figure S4

Detection of CD57<sup>+</sup> B cells. (A) Reverse cumulative distributions of CD57 mass cytometry signal in B cells, with red curves representing run1 patients, blue run2 patients and green run2 healthy control. (B) Flow cytometry data for five SLE patients at baseline, selected by high CD57 frequency in mass cytometry data. Numbers above square gates show percentages, while numbers in the top left denote patient IDs. Gating strategy from patient 10 is shown below, including lymphocyte gating followed by doublets, CD3<sup>+</sup>, CD16<sup>+</sup> and dead cells exclusion; afterwards CD19<sup>+</sup> B cells were selected. (C) Violin plots depicting the grade of marker expression (yellow) on the combined B cell clusters #6 and #25 delineated in Figure 1B. The marker expression on the remaining B cells is also displayed for comparison (pink). Width indicates the frequency of the expression level shown on the y-axis.

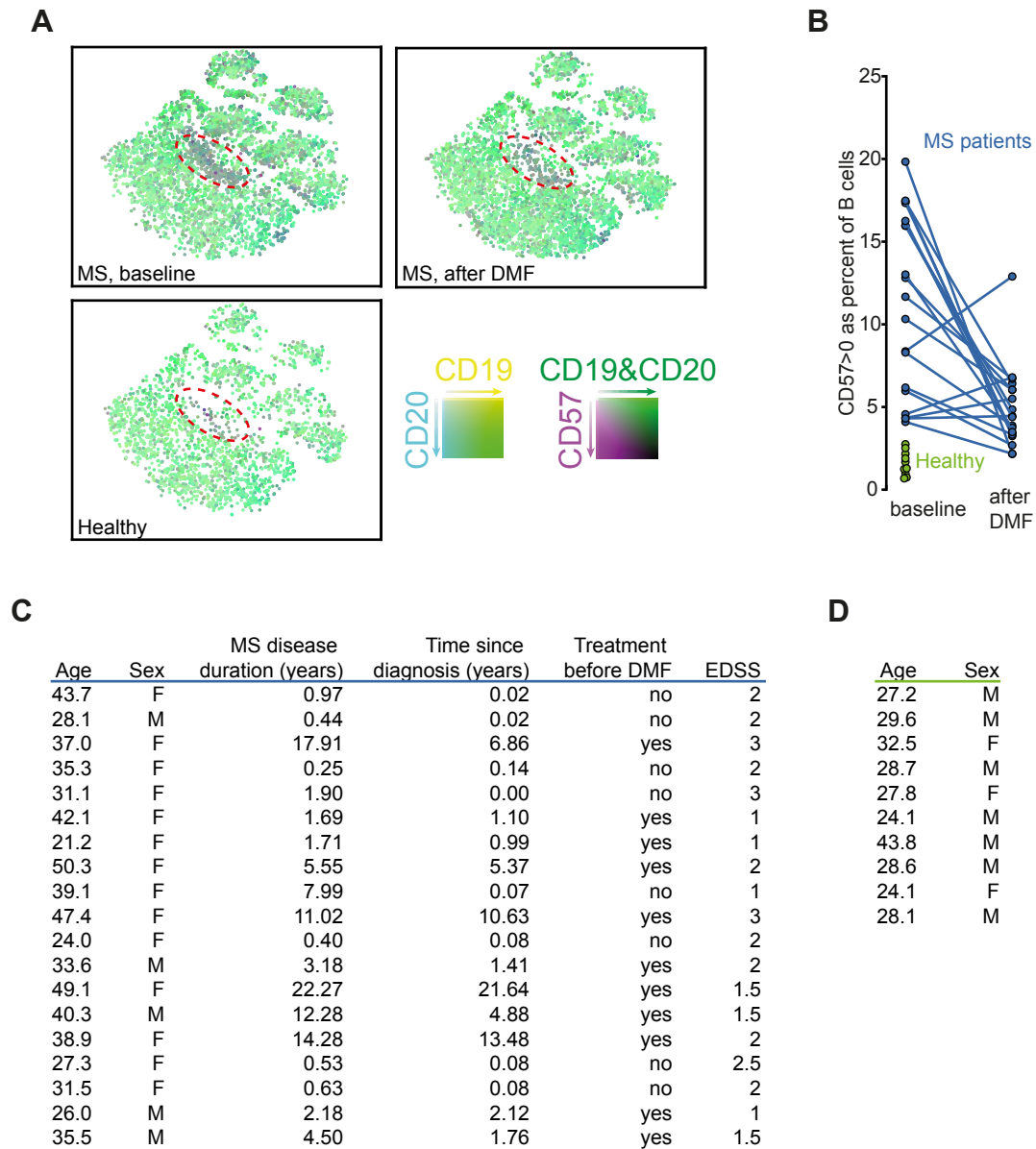


**Figure S5**

B cell CD57 expression in healthy and MS individuals. This figure shows B cell mass cytometry data from 19 multiple sclerosis (MS) patients before and after treatment with dimethyl fumarate and 10 healthy controls. (A) CD19, CD20 and CD57 signal scaled to the maximum for each protein for 160 cells per patient sample (and 300 per healthy, since fewer such individuals were included) arranged by t-SNE and CD57-rich cluster marked by a red oval. (B) The percentage of B cells that give any CD57 signal. (C) Baseline characteristics for MS patients, with one row each. (D) Age at time of sampling and sex of healthy controls, with one row each.

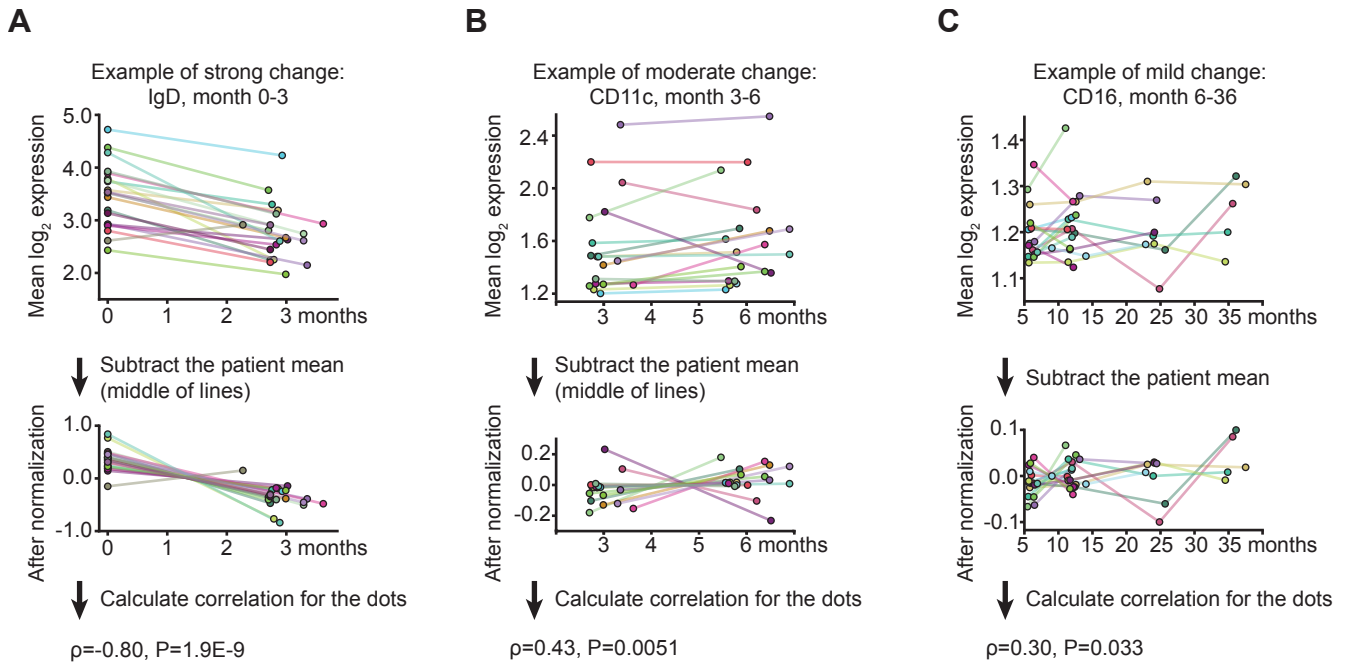


**Figure S6**

Examples of marker changes. (A–C) Steps of normalisation to the mean are demonstrated for each marker and each patient to extract the Spearman's rank correlation coefficients for correlations of individual marker expressions with time on treatment demonstrated in Figure 3. Examples of strong (A), moderate (B) and mild (C) expression changes are illustrated.

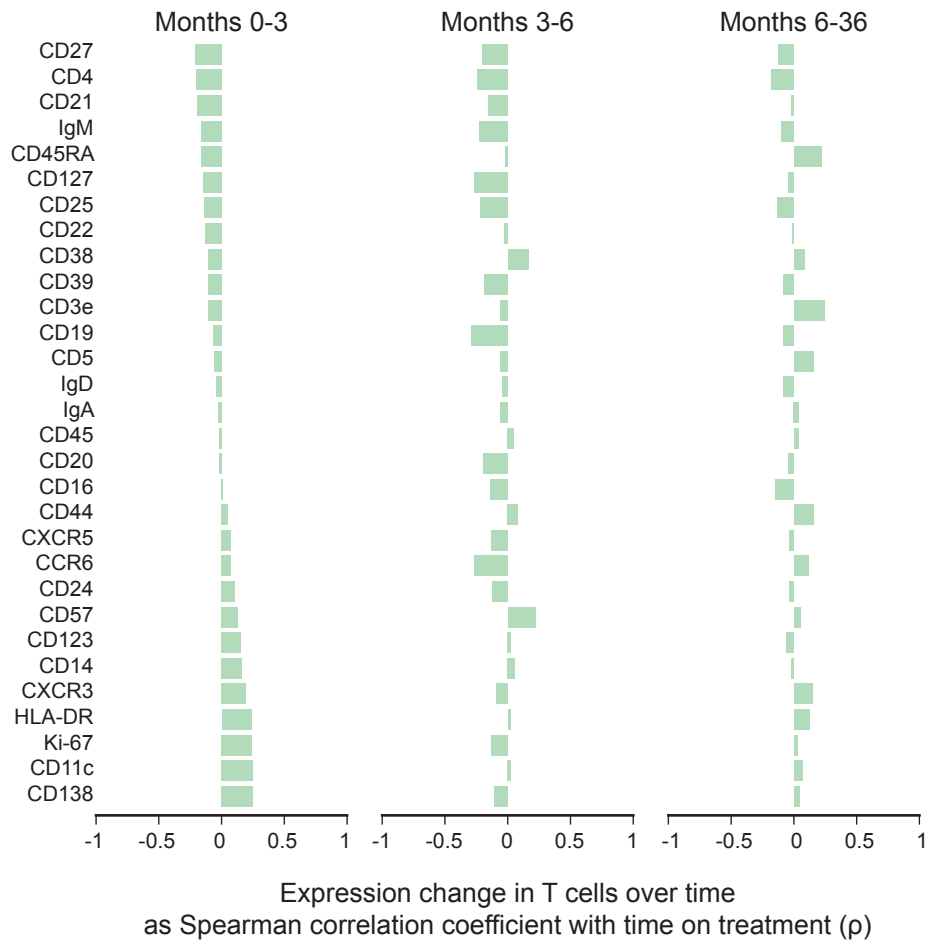


**Figure S7**

Marker expression changes on T cells. Changes of individual cell surface antigen expression on T cells during follow-up. Spearman's rank correlation coefficients for correlations of each antigen with time on treatment are demonstrated for early (months 0–3), intermediate (months 3–6) and late (months 6–36) alterations.

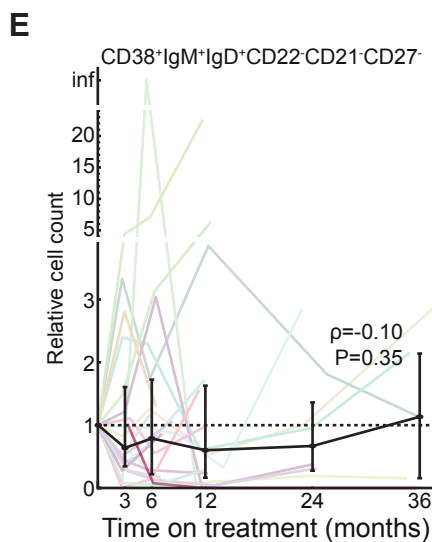
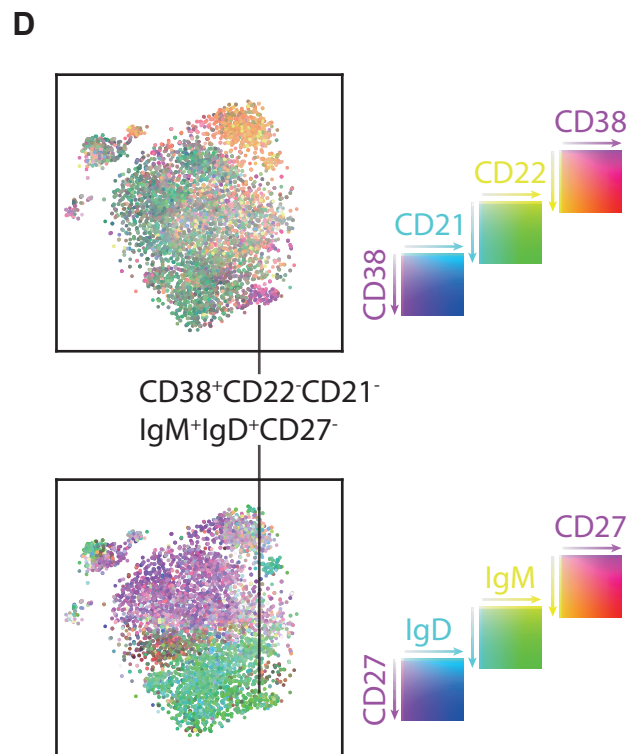
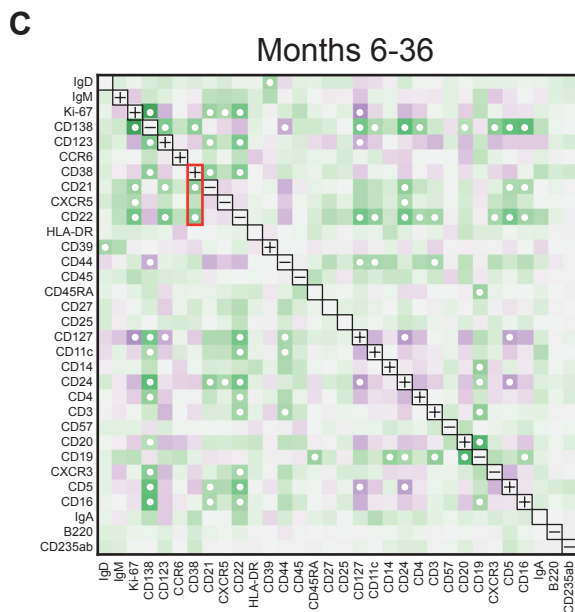
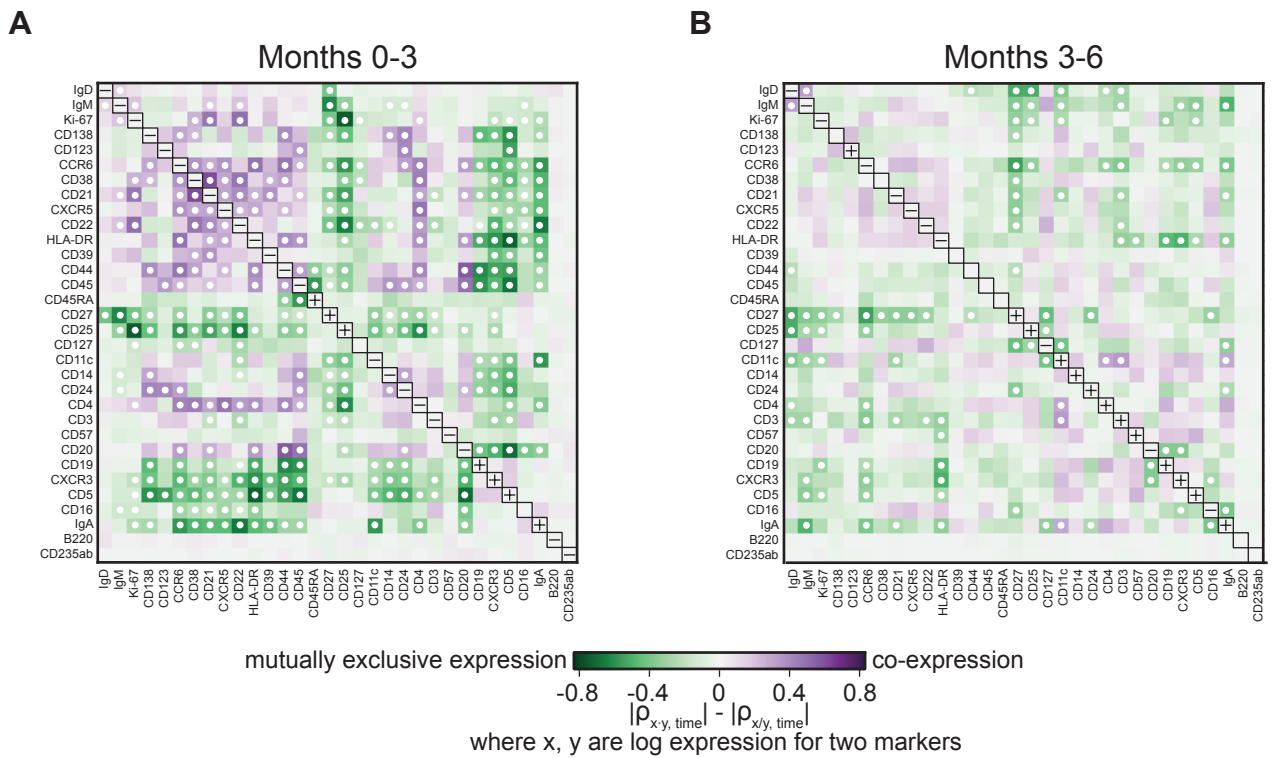


**Figure S8**

Paired marker expression for all markers included in the panel. (A–C) Paired marker expression for early (months 0–3; A), intermediate (months 3–6; B) and late (months 6–36; C) alterations. Colour intensity represents the difference between correlations of co-expression and mutually exclusive expression of marker pairs with time on treatment. Dots denote significant differences ( $P < 0.05$ ) of cell subsets co-expressing or mutually lacking the respective marker pairs. While CD38 was strongly co-expressed with CD21 and CD22 at early time points (Figure 3C), it showed a mutually exclusive expression pattern with CD21 and CD22 at later time points (C). (D–E) A  $CD38^+IgM^+IgD^+CD22^-CD21^-CD27^-$  B cell subset can be observed, this best corresponds to transitional type 1 B cells (D). This subset was found to be resistant to belimumab treatment (E). Colored lines in E show patients separately.



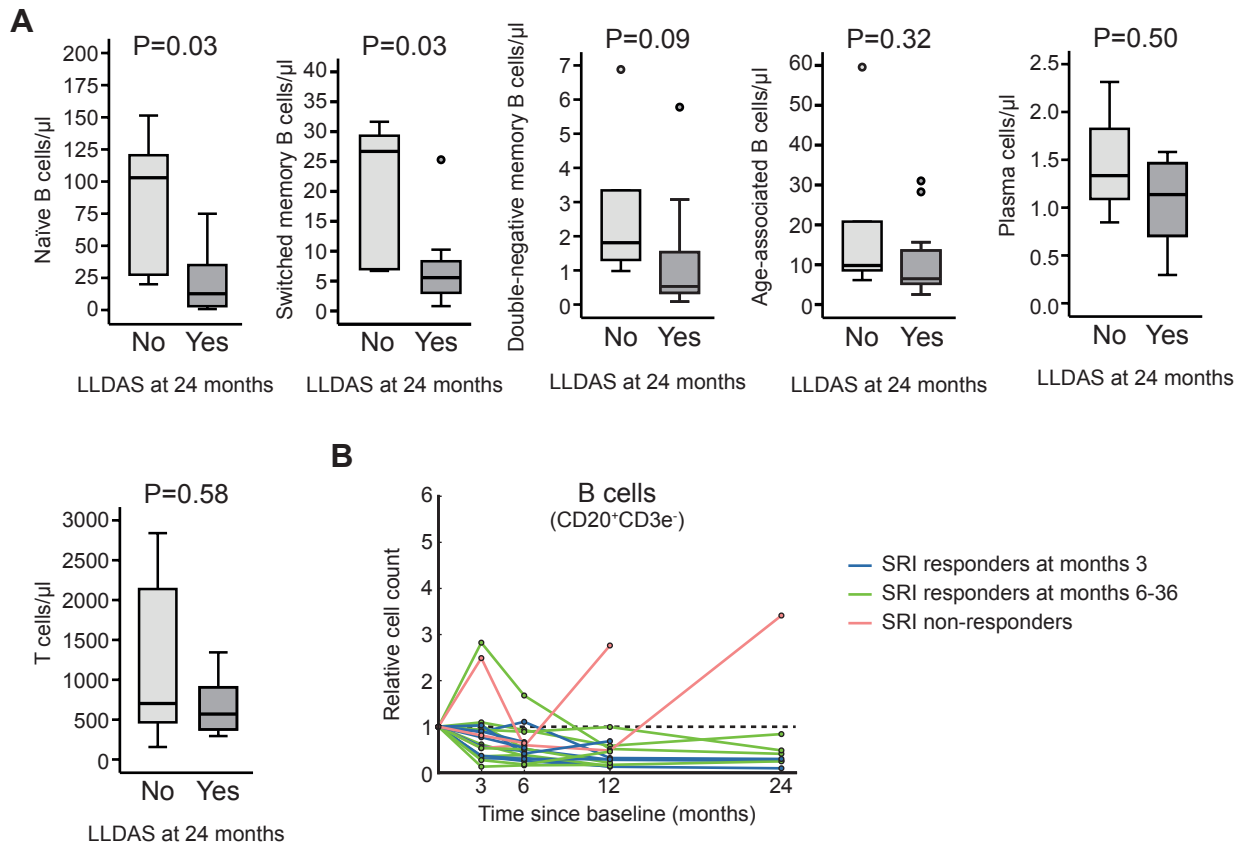


**Figure S9**

Cell counts in responders versus non-responders. (A) Comparisons of baseline cell counts for different lymphocyte subsets between patients who had clinical response as measured by LLDAS at month 24 and patients who had not. Box plots represent baseline cell count distributions. Lines in the boxes denote medians, bounds denote quartiles, whiskers denote ranges and circles denote out or extreme values. (B) B cell alterations during follow-up in early responders, late responders and non-responders as measured by SRI.

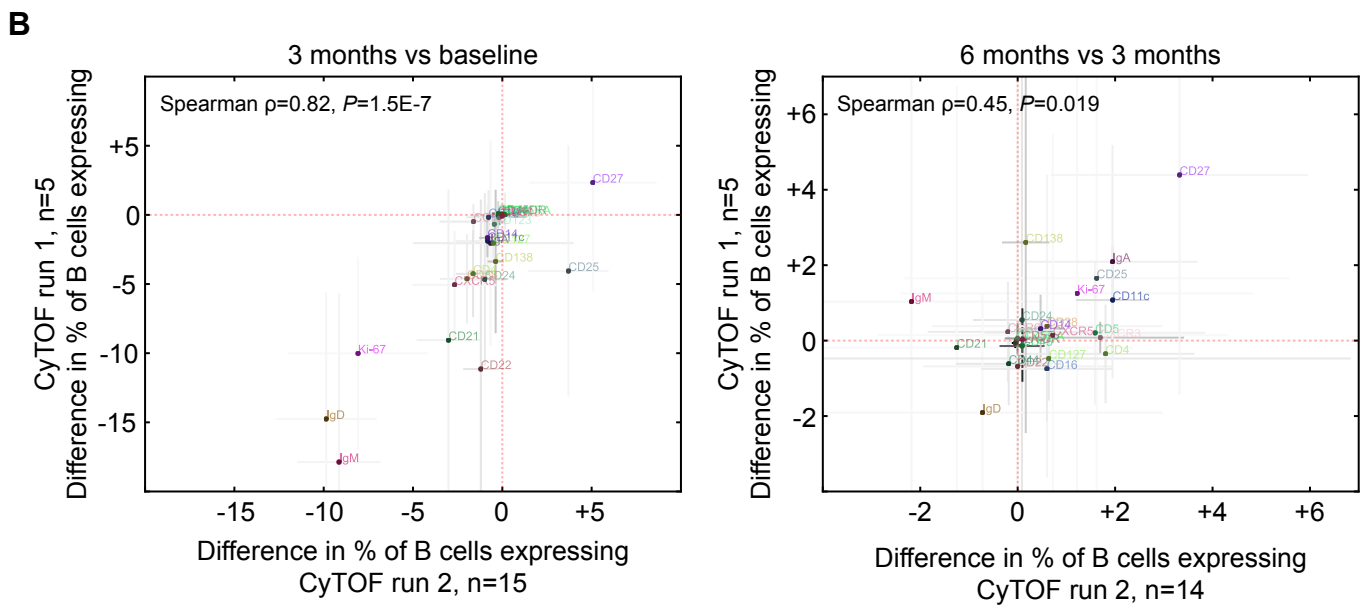
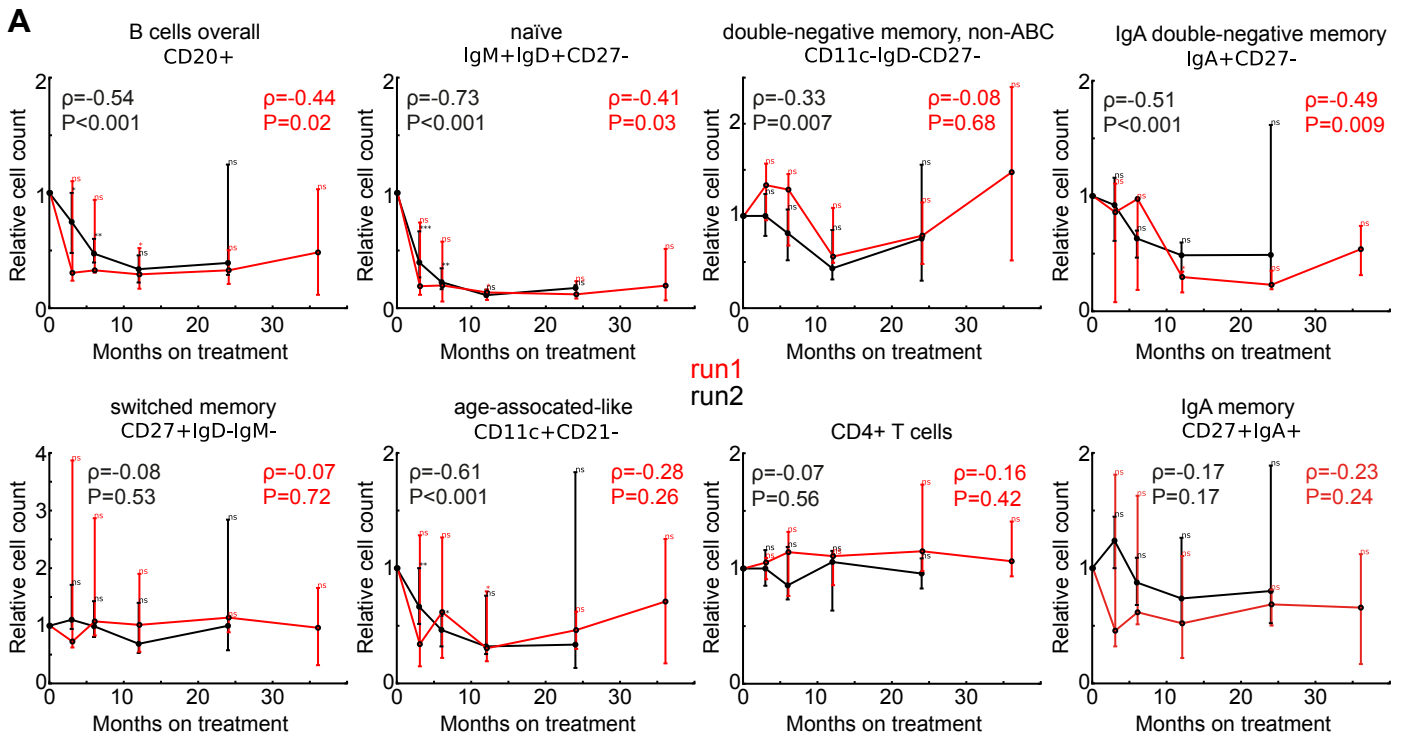


**Figure S10**

Concordance between the run1 and run2 cohorts. (A) Relative cell count alterations in predefined B and T cell subsets on each follow-up occasion compared to baseline values, with lines representing medians and error bars representing quartiles. Spearman's rank correlation coefficients ( $\rho$ ) for correlations of cell populations with time from baseline and the corresponding P-values are shown in the respective graphs. The colors show the first (red) and second (black) machine runs.

\* $P < 0.05$ , \*\* $P < 0.01$ , \*\*\* $P < 0.001$ , ns  $P > 0.05$ , compared to baseline. Only timepoint with  $n \geq 3$  included, see Figure 1A for n.

(B) Scatterplot of the slopes for each marker's values between two timepoints for the two cohorts. Error bars show 95% confidence intervals.

<b>Metal tag</b>	<b>Antigen</b>	<b>Clone</b>	<b>Vendor</b>	<b>Cat Number</b>
Y89	CD45	HI30	Fluidigm	3089003B
In113	CD235a/b*	HIR2	Fluidigm	306602
In115	CD57	HCD57	BioLegend	322302
Pr141	CCR6 (CD196)	G034E3	Fluidigm	3141003A
Nd142	CD19	HIB19	Fluidigm	3142001B
Nd143	CD5	UCHT2	BioLegend	300602
Nd144	CD16	3G8	BioLegend	302002
Nd145	CD138	DL-101	Fluidigm	3145003B
Nd146	IgM	MHM-88	BioLegend	314502
Sm147	CD11c	Bu15	Fluidigm	3147008B
Nd148	IgA	Polyclonal	Fluidigm	3148007B
Sm149	CD25	2A3	Fluidigm	3149010B
Eu151	CD123	6H6	BioLegend	306002
Sm152	CD21	BL13	Fluidigm	3152010B
Sm154	CD3e	UCHT1	Fluidigm	3154003B
Gd155	CD22	HIB22	BioLegend	302502
Gd157	CD183 (CXCR3)	G025H7	BioLegend	353702
Tb159	CD4	RPA-T4	BioLegend	300502
Gd160	CD14	M5E2	BioLegend	301802
Dy161	CD24	ML5	BioLegend	339902
Dy162	Ki-67	B56	Fluidigm	3162012B
Dy163	HLA-DR	L243	BioLegend	307602
Dy164	CD44	BJ18	BioLegend	338802
Ho165	CD127 (IL-7R $\alpha$ )	A019D5	Fluidigm	3165008B
Er167	CD27	L128	Fluidigm	3167006B
Er168	CD38	HIT2	BioLegend	303502
Tm169	CD45RA	HI100	Fluidigm	3169008B
Er170	CD20	2H7	BioLegend	302302
Yb172	IgD	IA6-2	BioLegend	348202
Yb173	CD39 <sup>†</sup>	A1	BioLegend	328202
Yb173	CD45R/B220*	RA3-6B2	BioLegend	103202
Yb174	CD185 (CXCR5)	51505	R&D Systems	MAB190
Ir191	Cell-ID <sup>™</sup> Intercalator-Ir (DNA)	-	Fluidigm	201192A
Ir193	Cell-ID <sup>™</sup> Intercalator-Ir (DNA)	-	Fluidigm	201192A
Pt195	Cell-ID <sup>™</sup> Cisplatin (Live-dead)	-	Fluidigm	201064
*Only used in experiment number 1 (5 patients).				
†Only used in experiment number 2 (18 patients), instead of CD45R/B220.				

**Table S1.** Mass cytometry panel

<b>Dye</b>	<b>Antigen</b>	<b>Clone</b>	<b>Vendor</b>	<b>Notes</b>
PerCPCy5.5	CD3	SK7	BD Biosciences	7AAD in same channel
BV421	CD19	HIB19	BD Biosciences	
BV510	CD20	L27	BD Biosciences	
BV605	IgD	IA6-2	BD Biosciences	
BV786	CD27	L128	BD Biosciences	
PE-Cy7	CD38	HIT2	BD Biosciences	
FITC	CD57	HCD57	BioLegend	
BUV395	CD11c	B-ly6	BD Biosciences	
BUV737	CD21	B-ly4	BD Biosciences	
APC	IgA	IS11-8E10	Miltenyi Biotec	
APC-H7	CD14	MφP9	BD Biosciences	

**Table S2.** Flow cytometry panel